JOURNAL OF PROPULSION AND POWER
Vol. 11, No. 4, July–August 1995

Magnetic Field Control of Burning Rate and Thrust in Solid Rocket Motors

Igor G. Borovskoi* and Alexander B. Vorozhtsov†
Research Institute of Applied Mathematics and Mechanics, Tomsk 634050, Russia

A model is developed for a flow of ionized gaseous combustion products in a channel with conducting walls. The channel is exposed to an external uniform magnetic field oriented so that the direction of the induced ponderomotive force is opposite to the flow direction. This decreases the gas flow velocity and increases the static pressure. For condensed systems, wherein the mass burning rate is proportional to external pressure and burning surface temperature, the pressure rise leads to the increased rate of combustion product generation. The determining parameters are revealed by means of numerical analysis. The influence of these parameters on the combustion process in a rectangular channel is established. It is shown that a more than tenfold increase in burning rate is possible at moderate values of the parameter of magnetogasodynamic interaction. The theoretical background of the magnetic field control over the flow direction of combustion products is discussed. The essence of the method is in a certain orientation of the external magnetic field with respect to the flow of a conducting medium, which induces the ponderomotive force whose deviating component changes the direction of the flow of combustion products in channels of various configurations. The degree of deviation of a three-dimensional gas flow in an axisymmetric de Laval nozzle exposed to a one-dimensional uniform magnetic field is considered.

Nomenclature

$\boldsymbol{A}, \boldsymbol{C}, \boldsymbol{F}$ = column vectors
$\boldsymbol{B}$ = vector of magnetic flux density, N/(A·m)
b = half of channel height, m
c_f = friction stress
c_p = specific heat, J/(kg·K)
d = const, Eq. (20), m/s
E = volumetric specific total energy, J/kg
e_c = dimensionless parameter
$\boldsymbol{f}$ = vector of ponderomotive force, N/m³
Ha = Hartmann number
h = total enthalpy of gas flow, J/kg
$\boldsymbol{j}$ = vector of electric current density, A/m²
k = ratio of the nozzle outlet section to the nozzle throat
L_e = coordinate of outlet section, m
L_{MF} = length of magnetic field region, m
M = Mach number
m = mass velocity, kg/(m²·s)
$\boldsymbol{n}$ = vector of outward normal to surface S
p = pressure, Pa
Q = energy, J/(m³·s)
R_x, R_y = components of a thrust vector, N
S = surface covering volume V, m²
St = Stanton number
T = temperature, K
t = time, s
$\boldsymbol{U}$ = gas velocity vector, m/s
u = components of a vector $\boldsymbol{U}$ in cylindrical coordinates
V = volume, m³
w = function in Eq. (24)
w_x, w_y = components of vector $\boldsymbol{U}$ in Cartesian coordinates
$\boldsymbol{x}, \boldsymbol{r}, \boldsymbol{\varphi}$ = basis vectors of cylindrical coordinates
$\boldsymbol{x}, \boldsymbol{y}, \boldsymbol{z}$ = basis vectors of Cartesian coordinates
α = heat exchange coefficient, W/(m²·K)
β = slope of magnetic field vector
γ = gas adiabate index
δ = slope of thrust vector
θ = T/T_g, dimensionless temperature
μ = dynamic viscosity, Pa·s
ν = burning rate pressure exponent
π = dimensionless pressure
ρ = density, kg/m³
σ = specific conductance, A/(V·m)
τ = time step, s
φ = dimensionless parameter
ψ = reduction coefficient of critical nozzle throat

Subscripts

c = condensed phase
d = dissipation
e = outlet section
g = gas phase
H = magnetic values
s = surface
w = impermeable
x, y, z, r, φ = corresponding coordinate components
0 = inlet section and undisturbed parameters
$*$ = boundary parameter
$\top$ = top
$\perp$ = bottom

Superscript

n = nth calculation cell at time t

Received Sept. 24, 1994; revision received Jan. 30, 1995; accepted for publication Feb. 6, 1995.

*Senior Researcher, Department of Gas Dynamics and Combustion.
†Professor, Head of Department of Gas Dynamics and Combustion.

Introduction

THE methods available for controlling propellant combustion and thrust in solid rocket motors are base mainly on mechanical principles.[1] The parts of the devices and units used in these methods are subject to strong thermochemical

and erosion effects of high-temperature two-phase flows, which can be detrimental to the reliability of the mechanisms and can take additional expense for their protection.

In this work, we suggest an alternative method for controlling the combustion of solid propellants, based on the effect of an external magnetic field on plasma flow. This principle has a wide application in such energy converters as magnetogasodynamic generators and pumps, and flowmeters, etc.[2,3] The effect of external magnetic field can be used in controlling the burning rate due to the fact that the combustion products of solid propellant at temperatures above 2000 K constitute an ionized gas. It has been shown that the specific conductance σ of combustion products depends on gas flow pressure and temperature, and is $\sigma = 0.1-1$ A/(V·m) for usual propellants, and $\sigma > 100$ A/(V·m) for plasma-generating formulations. All the results presented later were obtained assuming the constant specific conductance $\sigma = 50$ A/(V·m).

It is common knowledge that the combustion behavior of a solid propellant is determined by a number of parameters, including environmental pressure and burning surface temperature.[4] In this work, the effect of an external magnetic field on the burning rate of solid propellant is studied as a function of the above parameters. Problems concerned with changing the direction of the rocket motor thrust vector under the action of magnetic field are also considered.

Magnetic Field Effect on Gas Flow Pressure

A flow of ideal gas-ionized combustion products in a rectangular channel with conducting walls is investigated. Part of the channel is exposed to a uniform external magnetic field with no external electric field (Fig. 1). In the Cartesian coordinates, the velocity vector of the combustion products is $\boldsymbol{U} = (u_x, 0, 0)$ and the magnetic field is oriented so that the magnetic flux density vector $\boldsymbol{B}$ has only the transverse component $\boldsymbol{B} = (0, B_y, 0)$. For the channel inlet section ($x = 0$), we set the total enthalpy h_0 and the mass burning rate as a power function of pressure $m_0(p^\nu)$. For the outlet section ($x = L_e$), the external pressure p_e is given.

A detailed analysis of the electromagnetic part of a similar problem[3,5] has shown that the transverse magnetic field in the flow is also uniform. The bending of electric current lines due to crossing the boundaries of the magnetic field zone by the ionized gas flow is neglected. In this case (in the absence of electric field), electric currents are induced in the zone of magnetic field interaction with the gas flow.[5,6] It follows from generalized Ohm's law that the vector of electric current density $\boldsymbol{j}$ is equal to the vector product

$$\boldsymbol{j} = \sigma[\boldsymbol{U} \times \boldsymbol{B}] \tag{1}$$

and has one transverse component $\boldsymbol{j} = (0, 0, j_z)$, $j_z = \sigma u_x B_y$. Hence, the electric currents in gas circulate across the channel axis (Fig. 1) and short to the conducting wall of the channel.

The effect of the electric currents induced by the external magnetic field gives rise to a ponderomotive force $\boldsymbol{f}$ with its volume density vector

$$\boldsymbol{f} = [\boldsymbol{j} \times \boldsymbol{B}] \tag{2}$$

In this case the ponderomotive force has one component directly opposite to the $\boldsymbol{f} = (f_x, 0, 0)$, $f_x = -j_z B$.

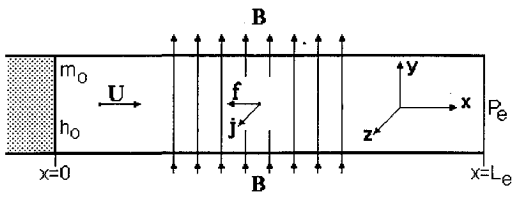

Fig. 1 Schematic diagram of a gas flow pattern.

Thus, in the magnetic field zone the combustion products are decelerated, which leads to a pressure rise upward the flow. As a result, the mass burning rate increases. Changing the magnetic induction of the external field allows one to control the burning rate of solid propellants.

The numerical analysis of the process under consideration is based on the integral Euler equations[7] in the approximation of magnetic gasdynamics,[5] with the Reynolds number being much less than unity.

The system of equations includes the following:

conservation of mass

$$\frac{\partial}{\partial t}\int_V \rho \, dV + \oint_S m \, dS = 0 \tag{3}$$

conservation of momentum

$$\frac{\partial}{\partial t}\int_V \rho \boldsymbol{U} \, dV + \oint_S (m\boldsymbol{U} + p\boldsymbol{n}) \, dS = \int_V \boldsymbol{f} \, dV \tag{4}$$

conservation of total energy

$$\frac{\partial}{\partial t}\int_V \rho E \, dV + \oint_S \left(E + \frac{p}{\rho}\right) m \, dS = \int_V (Q_f + Q_d) \, dV \tag{5}$$

where $m = \rho(\boldsymbol{U}\cdot\boldsymbol{n})$ is the mass rate of gas flow and

$$E = [p/\rho(\gamma - 1)] + 0.5|\boldsymbol{U}|^2 \tag{6}$$

is the volumetric specific total energy.

The steady-state solution of Eqs. (3–5) constitutes the initial conditions, and the boundary conditions are

$$x = 0: \quad m = \rho U_x = m_0(p^\nu) \tag{7}$$

$$x = 0: \quad E + (p/\rho) = h_0 \tag{8}$$

$$x = L_e: \quad p = p_e \tag{9}$$

Note that the right side of energy Eq. (5), consisting of the work of ponderomotive force Q_f and the Joule dissipation Q_d,[3,5] is equal to zero in the absence of external electric field. The work of $\boldsymbol{f}$ equals the scalar product

$$Q_f = (\boldsymbol{U}\cdot\boldsymbol{f}) \tag{10}$$

and, including Eq. (2)

$$Q_f = (\boldsymbol{U}\cdot[\boldsymbol{j} \times \boldsymbol{B}]) = -(\boldsymbol{j}\cdot[\boldsymbol{U} \times \boldsymbol{B}]) \tag{11}$$

The Joule heat, taking into account generalized Ohm's law (1), is

$$Q_d = (1/\sigma)(\boldsymbol{j}\cdot\boldsymbol{j}) = (\boldsymbol{j}\cdot[\boldsymbol{U} \times \boldsymbol{B}]) \tag{12}$$

Since $Q_f + Q_d \equiv 0$, the energy interaction is absent and the ionized gas flow is forced only by external magnetic field.

The use of the integral formulation of problems (3–5) is advantageous when solved numerically by the method of reference volume, i.e., Kolgan's modification[8] of the explicit Godunov's scheme[9] with the first-order approximation with respect to time and the second-order approximation with respect to spatial variables.

In terms of the reference volume method, regardless of the dimensional representation of the problem and the coordinates, the calculated flow parameters in the center of a calculation cell, an elementary volume, are determined through convective flows at the surfaces enclosing the cell.

The finite difference scheme can be obtained immediately from integral laws of conservation (3–5), using for brevity the column vectors $\boldsymbol{A}$, $\boldsymbol{C}$, and $\boldsymbol{F}$ for the sake of brevity:

$$\frac{\partial}{\partial t}\int_V \mathbf{A}\,dV + \oint_S \boldsymbol{C}\,dS = \int_V \boldsymbol{F}\,dV \tag{13}$$

$$\boldsymbol{A} = \begin{bmatrix}\rho\\ \rho U\\ \rho E\end{bmatrix}, \quad \boldsymbol{C} = \begin{bmatrix}m\\ mU + pn\\ m(E + p/\rho)\end{bmatrix}, \quad \boldsymbol{F} = \begin{bmatrix}0\\ f\\ 0\end{bmatrix} \tag{14}$$

It is assumed that the parameters attributed to calculation cell volumes and constituting column vector $\boldsymbol{A}$ are piecewise constant space functions. Then, the transformations

$$\frac{\partial}{\partial t}\int_V A\,dV = \frac{\partial}{\partial t}(AV)^n \cong V^n\frac{\boldsymbol{A}^{n+1} - \boldsymbol{A}^n}{\tau} \tag{15}$$

become valid. Upper index $n + 1$ corresponds the values at a time $t + \tau$, and the index n indicating the same parameters at a time t. Assuming the components of $\boldsymbol{C}$ constant, integration over the surface is replaced with summation, which provides the explicit difference scheme for determining the flow parameters through the convective flows of mass, momentum, and enthalpy:

$$\boldsymbol{A}^{n+1} = \boldsymbol{A}^n + \frac{\tau}{V^n}\left[F^n - \sum_S (CS)^n\right] \tag{16}$$

Operator Σ denotes summation of the entire limiting surface S^n, including the areas permeable and impermeable to gas, S_g^n and S_w^n, respectively.

Convective flows at interface S_g^n between two neighboring cells are determined by solving the problem of the decay of an arbitrary discontinuity.[9] Because of the impermeability of surface S_w^n the mass and enthalpy flows are identically equal to zero, and the momentum flow projections can be determined from the pressure at S_w^n, which is calculated by the formulas of "symmetric" decay of discontinuity.[9]

Boundary conditions can also be provided using the solution of the problem of arbitrary discontinuity decay. The parameters of convective flows at the inlet boundary are determined from the dependence $u_x^*(p^*)$ constructed using Eqs. (7) and (8); asterisks mark boundary parameters. This dependence is set equal to the relationship for the contact expansion rate $u_x^*(p^*, p^n, p^n, \rho^n, u_x^n)$, where the superscript n denotes gas parameters in the center of the calculation cell adjacent to the plane $x = 0$ at time t. Solution of the nonlinear equation yields the desired values of p^* and u_x^* at the inlet boundary; the density ρ^* is then determined by Eq. (8). The value of u_x^* at the outlet section is found from the relationship for contact discontinuity expansion rate, using the available pressure $p = p_e$. All possible configurations of the flow following a shock or rarefaction wave are then analyzed depending on the ratio of p^* to the pressure in the center of the cell adjacent to the plane $x = L_e$. This calculation procedure allows taking into account both subsonic and sonic flows through the outlet surface.

For the most part, the calculation scheme described above is consistent with the principles developed by Godunov.[9] In Kolgan's approach,[8] the parameters in each calculation cell are considered piecewise linear space functions rather then piecewise constant. In this case, the problem of arbitrary discontinuity decay is solved using a set of auxiliary values calculated by equations suggested by Kolgan.[8]

Calculations were performed for combustion products with $\gamma = 1.2$, the constant specific conductance $\sigma = 50$ A/(V·m) at $h_0 = 4$ MJ/kg, $\nu \in [0, 0.8]$, and external pressure $p_e = 0.1$ MPa.

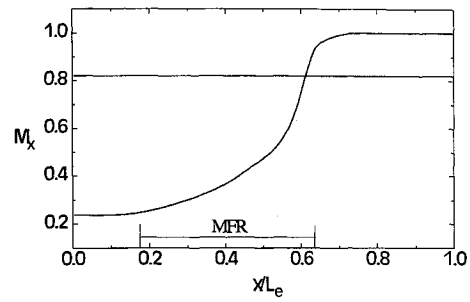

Fig. 2 Distribution of the Mach number in a channel exposed to external magnetic field for $S_H = 1$ and $\nu = 0.8$. MFR, magnetic field region.

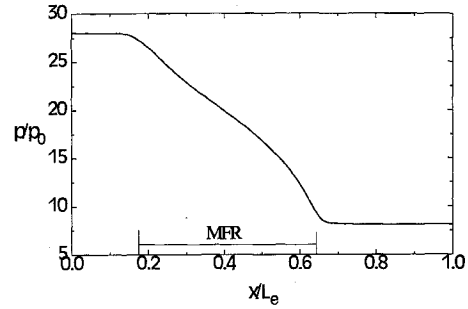

Fig. 3 Pressure distribution in a channel exposed to external magnetic field for $S_H = 1$ and $\nu = 0.8$. MFR, magnetic field region.

Typical stationary distributions of flow parameters for $\nu = 0.8$ are shown in Figs. 2 and 3. Initially, the flow of solid propellant combustion products is subsonic, its Mach number being $M_x = 0.82$ (dashed line in Fig. 2) at a constant static pressure p_e. It corresponds to the exact solution for an adiabatic flow of a nonviscous gas in a rectangular channel of constant cross section. The application of an external magnetic field decelerates the gas flow and leads to a more than twentyfold increasing pressure (Fig. 3), which increases the mass supply of combustion products. As a result, in the region following the magnetic field zone, the flow regime becomes sonic (Fig. 2), which corresponds to the exact solution for a flow in a constant cross section channel and can provide the validity of the results obtained in terms of the accepted model.

To account for the high sensitivity of the pressure in the chamber to the external magnetic field, we consider another way to change the mass burning rate in solid rocket motors, namely, by varying the nozzle throat. Writing mass balance in the combustion chamber for two throat values and dividing the equations term by term, we obtain

$$\pi^\nu = \pi\psi \tag{17}$$

where π is the coefficient of static pressure rise and ψ is the reduction coefficient of critical nozzle throat.

The latter equation suggests that

$$\pi = \psi^{-1/(1-\nu)} \tag{18}$$

Reducing the throat area, e.g., by a factor of 2 ($\psi = 0.5$), for $\nu = 0.8$ we then have a thirty-two-fold increase in pressure in the combustion chamber. A similar effect takes place in the magnetogasodynamic method when the flow of combustion products is decelerated in the zone of the external magnetic field effect.

An analysis of the stationary solution obtained from the balance analogs (lumping solutions) of Eqs. (3–5) shows that the relative mass supply m_H/m_0, i.e., the ratio of mass burning rates in the presence of and without the magnetic field, depends on the pressure exponent ν and on the parameter of

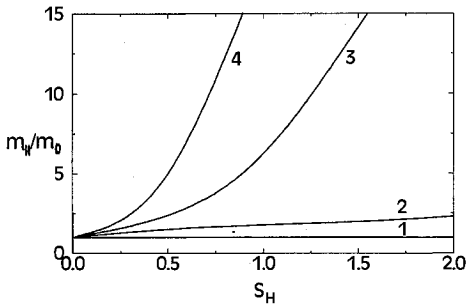

Fig. 4 Plots for dimensionless mass burning rate vs S_H at different ν. ν = 1) 0, 2) 0.4, 3) 0.6, and 4) 0.8.

magnetogasodynamic interaction S_H, which determines the relationship between the magnetic and inertial forces and is equal to

$$S_H = \sigma|\boldsymbol{B}|^2 L_{MF}/m_0 \tag{19}$$

where L_{MF} is the length of the channel section exposed to the external magnetic field.

The dimensionless burning rate of a solid propellant as a function of ν and S_H is shown in Fig. 4. As expected, the effect of the external magnetic field increases with ν. It is noteworthy that for $\nu > 0.6$, a more than tenfold increase in the mass supply of combustion products is possible at moderate S_H values.

The desired value of the magnetic flux density of the external magnetic field for the problem considered previously can be estimated using Eq. (19) and setting $S_H = 1$, $\sigma = 50$ A/(V·m), $m_0 = 2$ kg/(m²·s), and $L_{MF} = 0.1$ m, which yields $B_y \approx 0.6$ N/(A·m).

Magnetic Field Effect on Heat Exchange at the Burning Surface

A laminar flow of a noncompressible conducting medium in a high plane channel of height $2b$ exposed to a transverse uniform magnetic field is considered (Fig. 5). The bottom and top walls of the channel are the burning surfaces of a solid propellant, the conducting lateral walls being shorted. The variation of channel height due to propellant consumption is ignored. The magnetic flux density vector in the Cartesian coordinates is $\boldsymbol{B} = (0, B_y, 0)$ and, as in the previous problem, has one component in the flow zone, B_y = const. The value of electric current density $\boldsymbol{j}$, according to generalized Ohm's law, also has one component $j_z = \sigma u_x B_y$, with electric currents shorting to the lateral walls of the channel and the ponderomotive force vector, as previously, opposing the flow $\boldsymbol{f} = (f_x, 0, 0)$, $f_x = -j_z B_y$.

It follows from the solution of Hartman's problem for the considered flow in the absence of heat and mass exchange with the channel walls[5] that with other conditions being equal the increased magnetic induction of the external field leads to increased friction stress near the wall. Accepting the Reynolds assumption that the dynamic and thermal fields are similar for the given problem,[10] one should expect certain intensification of the heat transfer to the channel walls. This in turn can increase the surface temperature and burning rate since usually for solid propellants there is an exponential dependence of the mass burning rate m on the surface temperature θ_s at a constant pressure[11]

$$m(\theta_s) = d \exp[-(e_c/\theta_s)] \tag{20}$$

where $\theta_s = T_s/T_g$ is the ratio of the propellant surface temperature T_s to the gas temperature T_g in the flow core, d is constant, and the values of the dimensionless parameter e_c range within 0–3.[11]

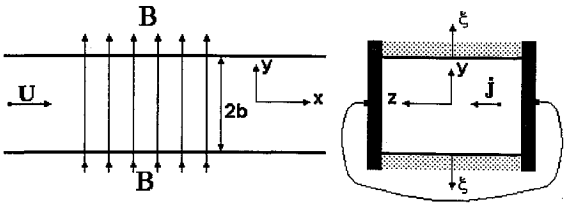

Fig. 5 Scheme of a flowfield in a rectangular channel.

The approximate value of magnetogasodynamic effect on burning surface temperature is estimated from the heat balance

$$\alpha = (T_g - T_s) = c_c m(T_s - T_\infty) \tag{21}$$

Dividing both sides of Eq. (21) by T_g and taking into account the Stanton number definition

$$St = \alpha/c_p m_g \tag{22}$$

where $m_g = m$ is the mass gas velocity in the flow core. After transformations we have

$$St \frac{c_p m_g}{c_c d} \frac{1 - \theta_s}{\theta_s - \theta_\infty} = \exp\left(-\frac{e_c}{\theta_s}\right) \tag{23}$$

Equation (23) applies both to the case with the magnetic field (in this case, the parameters are marked with the index H) and to the case without the magnetic field (index 0).

To estimate the Stanton number in the presence of the magnetic field, we use the solution of Hartmann problem

$$w(Ha) \equiv \frac{c_{f,H}}{c_{f,0}} = \frac{Ha^2}{3} \frac{th(Ha)}{Ha - th(Ha)} \tag{24}$$

where $c_{f,H}$ and $c_{f,0}$ are the dimensionless friction stresses at the wall with and without the magnetic field, respectively, and $th(Ha)$ is the hyperbolic tangent of the Hartmann number Ha, which is determined as follows[5]:

$$Ha = B_y b\sqrt{\sigma/\mu} \tag{25}$$

It has been shown by Loitsanskii[5] that, in general, the relative friction stress is a function of two variables, $w(Ha, \varphi)$. The dimensionless parameter φ incorporates the specific conductance coefficients of the walls and combustion products as well as the geometric characteristics of the channel, the dependence of $c_{f,H}/c_{f,0}$ on Hartmann number increasing with φ. In order to obtain a lower estimation for the effect of the magnetic field on heat-mass exchange at the burning surface we take φ as zero.

Then, substituting the Reynolds analogy, which in terms of Eq. (24) has the form $St_H/St_0 = w(Ha)$, into Eq. (23) we have the final equation

$$St_0' w(Ha) \frac{1 - \theta_s}{\theta_s - \theta_\infty} = \exp\left(-\frac{e_c}{\theta_s}\right) \tag{26}$$

where the Stanton number St_0' constitutes the heat exchange coefficient α_0 in the absence of the magnetic field, the constant d, and the specific heat coefficient of solid propellant c_c. This substitution is possible if the magnetic field-induced changes in the mass velocity of combustion products in the flow core (unlike the mass burning rate) are neglected, i.e., if it is assumed that $m_0 = m_H$.

Figures 6 and 7 show the numerical solution of nonlinear Eq. (27) at the dimensionless parameter ranging within $e_c \in [0, 2]$. The ratios $\theta_{s,H}/\theta_{s,0}$ and m_H/m_0 are independent of the

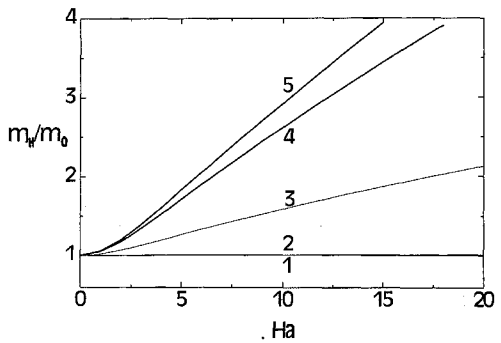

Fig. 6 Plots for dimensionless mass burning rate vs *Ha* and e_c. e_c = 1) 0, 2) 0.5, 3) 1.0, 4) 1.5, and 5) 2.0.

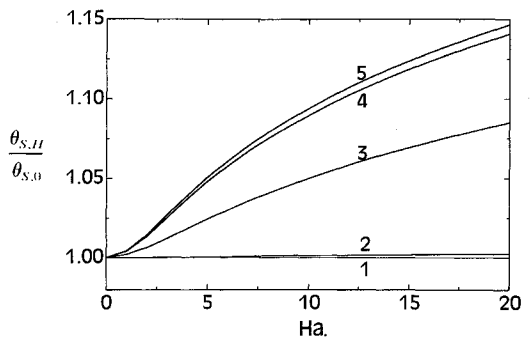

Fig. 7 Plots for dimensionless surface temperature of a solid propellant vs *Ha* at different e_c. e_c = 1) 0, 2) 0.5, 3) 1.0, 4) 1.5, and 5) 2.0.

Stanton number St'_0 and weakly dependent on the temperature θ_∞. The results obtained suggest that with increasing Hartman's number, the propellant surface temperature increment is 15% (at $Ha < 20$), while the burning rate shows more than twofold increase, accounted for by the exponential dependence in Eq. (20).

For the estimation of the required value of the magnetic induction of external field, it is assumed that $Ha = 10$, $\sigma = 50$ A/(V·m), $\mu = 5 \times 10^{-5}$ N·s/m^2, and $b = 0.1$ m. Thus, it follows from the Hartmans number definition that $B_y \approx 0.1$ N/(A·m).

The results presented are qualitative, and are indicative of the possible essential influence of an external magnetic field on the combustion of solid propellants. The authors did not extend the range of *Ha* variation at $m_H/m_0 > 1$, since the intense efflux from channel walls would violate the assumptions accepted in the approximation of both laminar and turbulent boundary layers.[10] Hence, Eq. (24), used as the basis for the present analysis, could also be violated. A detailed investigation of the problem can be performed and quantitative results can be obtained only by solving the complete Navier–Stokes equations for a compressible gas, supplemented by equations for diffusion and magnetic induction as well as by the appropriate sides responsible for the chemical reactions proceeding in the gas flow and at the burning surface.

Control of Thrust Vector Direction

The external magnetic field can also be applied to a flow of solid–propellant combustion products in order to deviate the flow of ionized gas from the longitudinal axis of the flow channel. In practice, this method may be employed, e.g., to change the direction of a conducting flow in pipe-line branching and to control the direction of the thrust vector in flying vehicles. A three-dimensional flow of ionized ideal gas is considered in a conic de Laval nozzle with conducting walls (Fig. 8). The velocity vector of combustion products U consists of

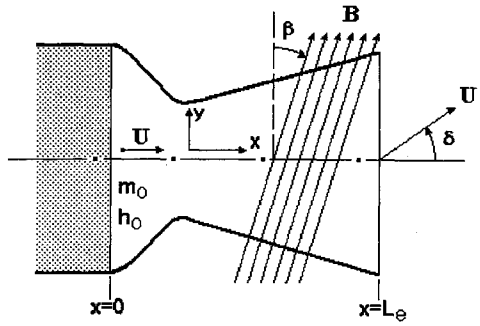

Fig. 8 Schematic diagram of a flowfield in a nozzle.

three components $U = (u_x, u_r, u_\varphi)$ in the cylindrical coordinates $\{x, r, \varphi\}$. The outlet section of the nozzle is exposed to a one-dimensional uniform magnetic field that is applied at such an angle with the nozzle axis that in the Cartesian coordinates $\{x, y, z\}$ the magnetic flux density vector has two components $B = (B_x, B_y, 0)$: $Bx = |B|\sin(\beta)$.

In solving the problem, it is more convenient to describe the flow using two systems of coordinates. The axisymmetric shape of the nozzle calls for the symmetric coordinates to describe the flow of combustion products, while the magnetic field effect is conveniently calculated in the Cartesian coordinates. The unidirectional unit vector x of both systems extends along the nozzle axis.

The constant values of mass burning rate m_0 and total enthalpy of gas h_0 are set for the inlet section of the channel ($x = 0$), and the external pressure $p_e = 0$ is specified for the outlet section. The gas flow is symmetric about the XY plane (Fig. 8).

As before, we disregard the end effects and assume the magnetic field to be uniform all through the interaction zone wherein electric currents are induced shorting to the nozzle walls. The electric current density vector $j = (0, 0, j_z)$ has one component $j_z = \sigma(w_x B_y - w_y B_x)$, where w_x and w_y are the components of the velocity vector U in the Cartesian coordinates. The interaction of the external field with the induced currents gives rise to a ponderomotive force $f = (f_x, f_y, 0)$, which, in this case, has two components: decelerating $f_x = -j_z B_y$, directed opposite to the gas flow, and deviating $f_y = j_z B_x$, orthogonal to the nozzle axis. The latter component deviates the flow of combustion products towards the top wall of the nozzle, increasing the pressure near this wall and rarefing the gas at the opposite wall.

The mathematical description of the motion of combustion products in the nozzle is based on the solution of Eqs. (3–5), with Eqs. (7–9) considered as boundary conditions, complemented by the relationships for the inlet section ($x = 0$), $u_r = 0$, and $u_\varphi = 0$. For supersonic flows, the boundary conditions for the outlet section ($x = L_e$) are not specified; in this case the flow parameters from the calculation cells adjacent to the outflow section are used. The problem was tested by comparison with available exact solutions for a conical nozzle[9] as well as with independent numerical results.[12] Comparison of calculated pressure distributions along the axis and in the vicinity of nozzle walls has demonstrated the high reliability of results obtained in the absence of magnetic field.

At $|B| \neq 0$ the velocity vector components were determined in the Cartesian coordinates $\{x, y, z\}$, and the ponderomotive force components f_x and f_y were calculated for all calculation cells. The values of f_x, f_r, and f_φ were then calculated in the cylindrical coordinates $\{x, r, \varphi\}$. They served as the right sides of scalar analogs of the vector law of momentum conservation [Eq. (4)].

A preliminary analysis shows that the desired solution of the problem depends essentially on the slope of magnetic field orientation β, the parameter of magnetogasodynamic interaction S_H, and the ratio k of the nozzle outlet section to the

nozzle throat. Let us describe the principal characteristic features of a three-dimensional flow in a de Laval nozzle under the action of a one-dimensional uniform magnetic field. Figure 9 shows isobars (lines of constant static pressure p related to inlet pressure p_0) in a symmetry plane for a steady-state flow. It can be seen that for the magnetic field orientation shown in Fig. 8, pressure rises at the top wall of the nozzle and decreases at the bottom wall due to the crossflow of gas within the supersonic section of the nozzle (Fig. 10). Increasing S_H enhances the flow asymmetry and decelerates the flow, which at $S_H > 1$ can result in the generation of a shock wave at the top wall of the nozzle. Figure 11 shows the slope δ of the thrust vector as a function of the magnetic field slope β for different k and S_H. The angle δ is determined by the axial R_x and transverse R_y components of the thrust vector, $\delta = \text{arctg}(R_y/R_x)$. The axial component R_x is calculated by the momentum of combustion products at the nozzle exit section:

$$R_x = \int_{S_{Le}} (\rho u_x^2 + p)_{Le}\, dS_{Le} \tag{27}$$

Here, dS_{Le} is the element of the outlet section of the nozzle and the transverse component R_y is determined by the difference of static pressures at the top $p_\top$ and bottom $p_\perp$ walls of the nozzle

$$R_y = \int_{S_w} (p_\top - p_\perp)\, dS_w \tag{28}$$

where dS_w is the element of the lateral surface projected onto the plane passing through normally the nozzle axis to the XY plane.

Figure 11 demonstrates that every k corresponds to a certain maximum slope δ of the thrust vector. The slope for $\beta = 0$ and 90 deg is $\delta = 0$ deg, because at $\beta = 0$ deg the ponderomotive force vector f has only one decelerating component, and at $\beta \to 90$ deg the resultant effect of the magnetic field on the flow is absent.

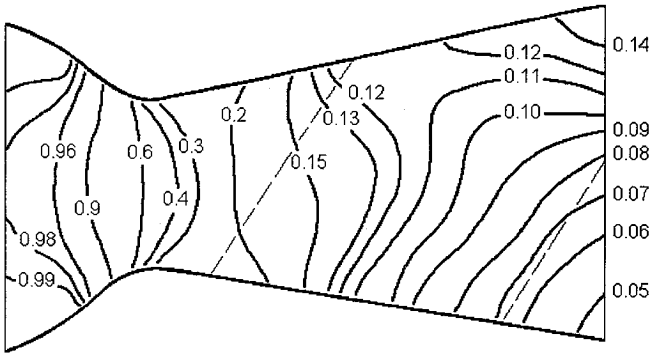

Fig. 9 Lines of a constant pressure in the symmetry plane at S_H = 0.5, k = 4, and β = 35 deg.

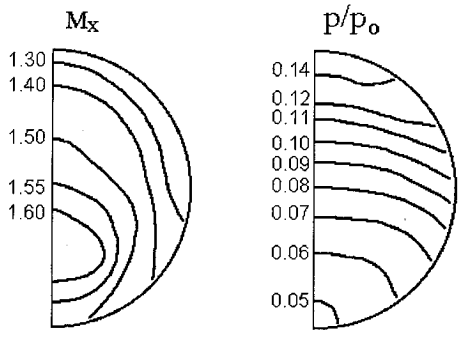

Fig. 10 Lines of constant pressure and the Mach number in the nozzle outlet section at S_H = 0.5, k = 4, and β = 35 deg.

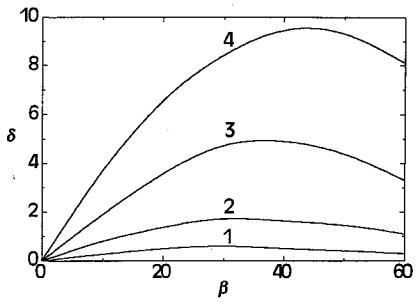

Fig. 11 Dependence of the gas flow deviation angle δ on β at different k and S_H. S_H = 1) 0.1, k = 4, 2) 0.1, k = 6.25, 3) 0.5, k = 4, and 4) 0.5, k = 6.

Conclusions

In this work, the possibility of controlling the mass burning rate of solid propellants and the direction of the combustion product flows by means of an external magnetic field is shown. Application of the magnetic field raises the gas pressure in the vicinity of the burning surface and increases the burning surface temperature. The effect can essentially lead to a manifold increase in the mass burning rate of solid propellant. It should be noted that in practice this method of contactless control can be very efficient since it involves no elements directly interacting with the high-temperature gas flow. The possibility of enhancing the efficiency of the method by introducing special ionizing additives into the gas flow to increase the specific conductance of combustion products should be emphasized. Such additives would allow one to control the burning rate at essentially lower magnetic induction values of the external field.

References

[1]Prisnyakov, V. F., *The Dynamics of Solid-Propellant Rocket Motors*, Mashinostroenie, Moscow, 1984.

[2]Vatazhin, A. B., Lyubimov, G. A., and Regirer, S. A., *Magnetohydrodynamic Flows in Channels*, Nauka, Moscow, 1970.

[3]Abramovich, G. A., *Applied Gas Dynamics*, Nauka, Moscow, 1976.

[4]Zenin, A. A., "Structure of Temperature Distribution in Steady-State Burning of a Ballistic Powder," *Combustion, Explosion and Shock Waves*, Vol. 2, No. 3, 1966, pp. 67–76.

[5]Loitsanskii, L. G., *Fluid and Gas Mechanics*, Nauka, Moscow, 1987.

[6]Parcell, E., *Electricity and Magnetism*, Nauka, Moscow, 1983.

[7]Sedov, L. I., *The Continum Mechanics*, Vol. 1, Nauka, Moscow, 1976.

[8]Kolgan, V. P., "Principle of Minimum Derivatives Applied to the Construction of Finite Difference Schemes for Discontinuous Solutions in Gas Dynamics," *Uchenye Zapiski TsAGI*, No. 6, 1972.

[9]Godunov, S. K., (ed.), *Numerical Solution of Multi-Dimensional Problems in Gas Dynamics*, Nauka, Moscow, 1976.

[10]Kutateladze, S. S., and Leont'ev, A. I., *Heat and Mass Transfer and Friction in Turbulent Boundary Layer*, Energoatomizdat, Moscow, 1985.

[11]Novozhilov, B. V., *Transient Combustion of Solid Propellants*, Nauka, Moscow, 1973.

[12]Davis, R. L., Ni, R. H., and Bowley, W. W., "Prediction of Compressible, Laminar Viscous Flows Using a Time-Marching Control Volume and Multiple-Grid Technique," *AIAA Journal*, Vol. 22, No. 11, 1984, pp. 1573–1581.